Results in Physics 4 (2014) 54–62

Contents lists available at ScienceDirect

Results in Physics

journal homepage: www.journals.elsevier.com/results-in-physics

Mixed convection flow of Eyring–Powell fluid along a rotating cone

S. Nadeem, S. Saleem *

Department of Mathematics, Quaid-i-Azam University 45320, Islamabad 44000, Pakistan

ARTICLE INFO

Article history:
Received 19 December 2013
Accepted 14 March 2014
Available online 22 March 2014

Keywords:
Heat transfer
Eyring–Powell fluid
Boundary layer
Optimal solutions

ABSTRACT

In the present article, we have studied the unsteady boundary layer flow of a rotating Eyring–Powell fluid on a rotating cone with the combined effects of heat and mass transfer. The governing momentum, energy and mass equations for unsteady flow are presented and simplified using similar and nonsimilar transformations. The reduced coupled nonlinear differential equations are solved analytically with the help of a strong analytical technique namely the optimal homotopy analysis method. Numerical results for important physical quantities are computed and displayed. The physical features of suitable parameters are discussed through the graphs of velocities, heat transfer, concentration, skin friction, Nusselt number and Sherwood number.

Introduction

Flow of non-Newtonian fluids has attained a great success in the theory of fluid mechanics due to its applications in biological sciences and industry. A few applications of non-Newtonian fluids are food mixing and chyme movement in the intestine, polymer solutions, paint, flow of blood, flow of nuclear fuel slurries, flow of liquid metals and alloys, flow of mercury amalgams and lubrications with heavy oils and greases. Some important studies of different non-Newtonian fluids studied by the researchers are cited in Refs. [1–9]. The phenomenon of mixed convection has fascinated most of the scientific experts due to its exclusive real world applications. Solar central receivers exposed to wind currents, electronic devices cooled by fans, nuclear reactors cooled during emergency shutdown, heat exchangers placed in a low velocity environment are some applications. In the pioneering work, Hering and Grosh [10] have investigated the steady mixed convection from a vertical cone for small Prandtl number. They applied similarity transformation which shows Buoyancy parameter is the dominant dimensionless parameter that would set the three regions, specifically forced, free and mixed convection. Himasekhar et al. [11] studied the similarity solution of the mixed convection flow over a vertical rotating cone in a fluid for a wide range of Prandtl numbers. Non-similar solutions to the heat transfer in unsteady mixed convection flows from a vertical cone were discussed by Kumari and Pop [12]. Anilkumar and Roy [13,14] presented the self-similar solutions of an unsteady mixed convection flow over a rotating cone in a rotating fluid. They found that similar solutions are only possible when angular velocity is inversely proportional to time. Non-similar solutions to the heat transfer in unsteady mixed convection flows from a vertical cone are presented by Ishak et al. [15]. Boundary layers on rotating cones, discs and axisymmetric surfaces with a concentrated heat surface have been studied by Wang [16]. Yih [17] inspected the mixed convection about a cone in a porous medium. Not a great attention has been paid to the three dimensional flows of Eyring–Powell fluid by the researchers. In fact this fluid model differentiates itself from other non-Newtonian fluid models. It is derived from kinetic theory of liquids in spite of empirical relation. Further it appropriately reduces to Newtonian behavior for low and high shear rates. Few studies regarding Eyring–Powell fluid are mentioned in Refs. [18–21].

The present article is a motivation of the above mentioned study. So we are concerned to examine the analytical solutions of unsteady mixed convective rotating flow of Eyring–Powell fluid in a rotating cone. The similarity solution is presented by using the optimal homotopy analysis method [22–33]. It is observed that similarity solutions are only possible when angular velocity is inversely proportional to time. At the end of the article, graphical and tabular results of some important physical quantities are discussed for some related parameters. Also the comparison of present results with the previous numerical results is computed as a special case of the present work.

Physical model

We are interested to investigate the unsteady laminar incompressible rotating flow of Eyring–Powell fluid over a rotating infinite cone. The coordinate system is considered to be fixed. The geometry of the flow problem is given in Fig. 1. The unsteadiness

* Corresponding author. Tel.: +92 3445510959.
E-mail address: salmansaleem_33@hotmail.com (S. Saleem).

http://dx.doi.org/10.1016/j.rinp.2014.03.004
2211-3797/

is introduced in the flow field due to the combined rotation of the fluid and the cone with the unsteady angular velocity in both directions i.e., (same or opposite). The wall and free stream are maintained at constant temperature and concentration. The buoyancy forces arise due to the temperature and concentration variations in the fluid. Further the flow is taken to be axisymmetric and also the dissipation effects are not considered.

The constitutive equation for a Cauchy stress in an Eyring–Powell model fluid is given by

$$\overline{\mathbf{S}} = \mu\nabla\overline{V} + \frac{1}{\beta}\sin h^{-1}\left(\frac{1}{c}\nabla\overline{V}\right)$$

where $\overline{V}$ is the velocity, $\overline{\mathbf{S}}$ is the Cauchy stress tensor, μ is the shear viscosity, β and c are the material constants. Considering

$$\sin h^{-1}\left(\frac{1}{c}\nabla\overline{V}\right) \approx \frac{1}{c}\nabla\overline{V} - \frac{1}{6}\left(\frac{1}{c}\nabla\overline{V}\right)^3, \quad \left|\frac{1}{c}\nabla\overline{V}\right| \ll 1.$$

After applying boundary layer and using the Boussinesq approximations, the governing equations for motion, temperature and concentration for Eyring–Powell fluid model are stated as

$$\frac{\partial u}{\partial x} + \frac{u}{x} + \frac{\partial w}{\partial z} = 0, \tag{1}$$

$$\begin{aligned}
&\frac{\partial u}{\partial t} + u\frac{\partial u}{\partial x} + w\frac{\partial u}{\partial z} - \frac{v^2}{x} = -\frac{v_e^2}{x} + g\beta\cos\alpha^*(T - T_\infty) \\
&+ g\beta^*\cos\alpha^*(C - C_\infty) + \left(\nu + \frac{1}{\rho\beta c}\right)\frac{\partial^2 u}{\partial z^2} \\
&- \frac{1}{6\rho\beta c^3}\left[\left(\frac{\partial u}{\partial z}\right)^2\left\{\frac{4}{x}\frac{\partial u}{\partial x} + \frac{2}{x}\frac{\partial w}{\partial z} + 4\frac{\partial^2 u}{\partial x^2} + 2\frac{\partial^2 w}{\partial x\partial z}\right\}\right. \\
&- \frac{\partial u}{\partial z}\frac{\partial v}{\partial z}\left\{\frac{3}{x}\frac{\partial v}{\partial x} + \frac{2v}{x^2} - 2\frac{\partial^2 v}{\partial x^2}\right\} + \frac{\partial u}{\partial z}\frac{\partial^2 u}{\partial z\partial x}\left\{16\frac{\partial u}{\partial x} + 8\frac{\partial w}{\partial z}\right\} \\
&- \left(\frac{\partial v}{\partial z}\right)^2\left\{\frac{2}{x}\frac{\partial w}{\partial z} + \frac{6u}{x^2} + \frac{2}{x}\frac{\partial u}{\partial x} + \frac{\partial^2 w}{\partial z\partial x}\right\} \\
&+ \frac{\partial v}{\partial x}\frac{\partial v}{\partial z}\left\{2\frac{\partial^2 w}{\partial z^2} + 4\frac{\partial^2 u}{\partial z\partial x}\right\}\frac{\partial^2 u}{\partial z^2}\left\{4\left(\frac{\partial u}{\partial x}\right)^2 + 4\frac{\partial u}{\partial x}\frac{\partial w}{\partial z} + \frac{v^2}{x^2}\right. \\
&+ \left(\frac{\partial v}{\partial x}\right)^2 - \frac{2v}{x}\frac{\partial v}{\partial x} + 4\left(\frac{\partial w}{\partial z}\right)^2\Big\} + \frac{\partial v}{\partial x}\frac{\partial^2 v}{\partial z^2}\left\{2\frac{\partial u}{\partial x} + \frac{2u}{x} + 2\frac{\partial w}{\partial z}\right\} \\
&+ \frac{\partial^2 v}{\partial x\partial z}\left\{\frac{2u}{x}\frac{\partial v}{\partial z} + 2\frac{\partial v}{\partial z}\frac{\partial w}{\partial z} - \frac{4v}{x}\frac{\partial u}{\partial z} + 4\frac{\partial u}{\partial z}\frac{\partial v}{\partial x} + 2\frac{\partial u}{\partial x}\frac{\partial v}{\partial z}\right\} \\
&+ \frac{\partial^2 v}{\partial z^2}\left\{-\frac{2uv}{x^2} + 2\frac{\partial v}{\partial z}\frac{\partial w}{\partial x} - \frac{2v}{x}\frac{\partial w}{\partial z} - \frac{2v}{x}\frac{\partial u}{\partial x}\right\} - \frac{4v}{x}\frac{\partial^2 u}{\partial x\partial z}\frac{\partial v}{\partial z} \\
&\left.+ \frac{\partial^2 w}{\partial z^2}\left\{-\frac{2v}{x}\frac{\partial v}{\partial z} + 8\frac{\partial u}{\partial z}\frac{\partial w}{\partial z} + \frac{\partial u}{\partial x}\frac{\partial u}{\partial z}\right\}\right]
\end{aligned} \tag{2}$$

$$\begin{aligned}
&\frac{\partial v}{\partial t} + u\frac{\partial v}{\partial x} + w\frac{\partial v}{\partial z} + \frac{uv}{x} = \frac{\partial v_e}{\partial t} + \left(\nu + \frac{1}{\rho\beta c}\right)\frac{\partial^2 v}{\partial z^2} \\
&- \frac{1}{6\rho\beta c^3}\left[\left(\frac{\partial u}{\partial z}\right)^2\left\{\frac{\partial^2 v}{\partial x^2} - \frac{3v}{x^2}\right\} + \frac{\partial^2 u}{\partial z\partial x}\left\{4\frac{\partial u}{\partial z}\frac{\partial v}{\partial x} - \frac{4v}{x}\frac{\partial u}{\partial z}\right.\right. \\
&+ \frac{2u}{x}\frac{\partial v}{\partial z} + 2\frac{\partial u}{\partial x}\frac{\partial v}{\partial z} + 2\frac{\partial v}{\partial z}\frac{\partial w}{\partial z}\Big\} + \frac{\partial^2 v}{\partial x\partial z}\left\{\frac{4u}{x}\frac{\partial u}{\partial z} + 2\frac{\partial u}{\partial x}\frac{\partial u}{\partial z}\right. \\
&- \frac{2v}{x}\frac{\partial v}{\partial z}\Big\} + \frac{\partial u}{\partial z}\frac{\partial v}{\partial z}\left\{\frac{2}{x}\frac{\partial u}{\partial x} + \frac{8u}{x^2}\right\} + \frac{\partial^2 u}{\partial z^2}\left\{2\frac{\partial u}{\partial x}\frac{\partial v}{\partial x} + 2\frac{\partial v}{\partial z}\frac{\partial w}{\partial x}\right. \\
&\left.\left.+ 2\frac{\partial v}{\partial x}\frac{\partial w}{\partial z} - \frac{2v}{x}\frac{\partial u}{\partial x} - \frac{2v}{x}\frac{\partial w}{\partial z} + \frac{2u}{x}\frac{\partial v}{\partial x} - \frac{2uv}{x^2}\right\}\right. \\
&+ \frac{\partial^2 v}{\partial z^2}\left\{2\frac{\partial u}{\partial z}\frac{\partial w}{\partial x} + \left(\frac{\partial v}{\partial x}\right)^2 + \frac{v^2}{x^2} - \frac{2v}{x}\frac{\partial v}{\partial x} + \frac{4u^2}{x^2} + \frac{4u}{x}\frac{\partial w}{\partial z}\right. \\
&+ 4\left(\frac{\partial w}{\partial z}\right)^2\Big\} + \frac{\partial^2 w}{\partial z^2}\left\{-\frac{2v}{x}\frac{\partial u}{\partial z} + \frac{4u}{x}\frac{\partial v}{\partial z} + 8\frac{\partial v}{\partial z}\frac{\partial w}{\partial z}\right\} \\
&\left.- \frac{\partial^2 v}{\partial z^2}\frac{\partial w}{\partial z} - \frac{\partial v}{\partial x}\frac{\partial^2 w}{\partial z^2} - \frac{2}{x}\frac{\partial u}{\partial z}\frac{\partial v}{\partial z} - \frac{\partial^2 u}{\partial x\partial z}\frac{\partial v}{\partial z} - \frac{\partial u}{\partial z}\frac{\partial^2 v}{\partial x\partial z}\right],
\end{aligned} \tag{3}$$

$$\frac{\partial T}{\partial t} + u\frac{\partial T}{\partial x} + w\frac{\partial T}{\partial z} = k\frac{\partial^2 T}{\partial z^2}, \tag{4}$$

$$\frac{\partial C}{\partial t} + u\frac{\partial C}{\partial x} + w\frac{\partial C}{\partial z} = D\frac{\partial^2 C}{\partial z^2}, \tag{5}$$

Employing the following similarity transformation [14]

$$\begin{aligned}
&v_e = \Omega_2 x\sin\alpha^*(1 - st^*)^{-1}, \quad \eta = \left(\frac{\Omega\sin\alpha^*}{\nu}\right)^{\frac{1}{2}}(1 - st^*)^{-\frac{1}{2}}z, \\
&t^* = (\Omega\sin\alpha^*)t, \quad u(t,x,z) = -2^{-1}\Omega x\sin\alpha^*(1 - st^*)^{-1}f'(\eta), \\
&v(t,x,z) = \Omega x\sin\alpha^*(1 - st^*)^{-1}g(\eta), \quad w(t,x,z) = (\nu\Omega\sin\alpha^*)^{\frac{1}{2}}(1 - st^*)^{-\frac{1}{2}}f(\eta), \\
&T(t,x,z) - T_\infty = (T_w - T_\infty)\theta(\eta), \quad T_w - T_\infty = (T_0 - T_\infty)\left(\frac{x}{L}\right)(1 - st^*)^{-2}, \\
&C(t,x,z) - C_\infty = (C_w - C_\infty)\phi(\eta), \quad (C_w - C_\infty) = (C_0 - C_\infty)\left(\frac{x}{L}\right)(1 - st^*)^{-2}, \\
&Gr_1 = g\beta\cos\alpha^*(T_0 - T_\infty)\frac{L^3}{\nu^2}, \quad Re_L = \Omega\sin\alpha^*\frac{L^2}{\nu}, \quad Pr = \frac{\nu}{\alpha}, \quad Sc = \frac{\nu}{D}, \\
&\lambda_1 = \frac{Gr_1}{Re_L^2}, \quad Gr_2 = g\beta\cos\alpha^*(C_0 - C_\infty)\frac{L^3}{\nu^2}, \quad \lambda_2 = \frac{Gr_2}{Re_L^2}, \\
&\alpha_1 = \frac{\Omega_1}{\Omega}, \quad N_1 = \frac{\lambda_2}{\lambda_1}, \quad R = \frac{1}{\mu\beta c}, \quad K = \frac{1}{6\mu\beta c^3}(\Omega\sin\alpha^*)^2(1 - st^*)^{-2}.
\end{aligned} \tag{6}$$

Here u, v and w are velocity components along x , y and z-axis, respectively, T is the temperature, K is the concentration, g is the gravity, k is the thermal diffusivity, D represents mass diffusivity, α^* is the semi-vertical angle of the cone, υ is the kinematic viscosity, ρ is the density, β and β^* are the volumetric coefficient of expansion for temperature and concentration, respectively, C_∞ and T_∞ are the free stream concentration and temperature, R and K are the flow parameters for Eyring–Powell model. By using the above mentioned similar and non-similar variables of Eq. (6), Eq. (1) is identically satisfied and Eqs. (2)–(5) give

$$\begin{aligned}
&(1 + R)f'''' - ff'' + 2^{-1}f'^2 - 2(g^2 - (1 - \alpha_1)^2) - 2\lambda_1(\theta + N\phi) \\
&- s(f' + 2^{-1}\eta f'') + K(8f'(f'')^2 - f''gg' + 4f'(g')^2 \\
&- 3(f')^2f'''' + 2f''''g^2) = 0,
\end{aligned} \tag{7}$$

$$\begin{aligned}
&(1 + R)g'' - (fg' - gf') + s(1 - \alpha_1 - g - 2^{-1}\eta g') \\
&+ K\left(\frac{1}{4}(f'')^2g + 12f'f''g' + 3(f')^2g'' - 2g(g')^2\right) = 0,
\end{aligned} \tag{8}$$

$$(Pr)^{-1}\theta'' - \left(f\theta' - f'\frac{\theta}{2}\right) - s\left(2\theta + 2^{-1}\eta\theta'\right) = 0, \tag{9}$$

$$(Sc)^{-1}\phi'' - \left(f\phi' - f'\frac{\phi}{2}\right) - s(2\phi + 2^{-1}\eta\phi') = 0. \tag{10}$$

$$\begin{aligned}
&f(0) = 0 = f'(0), \quad g(0) = \alpha_1, \quad \theta(0) = \phi(0) = 1, \\
&f'(\infty) = 0, \quad g(\infty) = 1 - \alpha_1, \quad \theta(\infty) = \phi(\infty) = 0.
\end{aligned} \tag{11}$$

where λ_1 is the buoyancy force, N is the ratio of the Grashof numbers. It vanishes for chemical diffusion, approaches to infinity for the thermal diffusion and positive when the buoyancy forces due to temperature and concentration difference act in the same direction and vice versa. s is the unsteady parameter and the flow is accelerating if $s > 0$ and the flow is decreasing, if $s < 0$. Further $\alpha_1 = 0$ shows that the fluid is rotating but the cone is at rest.

Moreover the fluid and the cone are rotating with equal angular velocity in the same direction for $\alpha_1 = 0.5$ and for $\alpha_1 = 1$, only the cone is rotating. The coefficient of local surface skin friction in x- and y-directions, the local Nusselt number and local Sherwood number in dimensionless forms are given by

$$\begin{aligned} C_{fx}Re_x^{\frac{1}{2}} &= [-(1+R)f'' - k\{(f')^2 f'' - 4f'gg'\}]_{\eta=0}, \\ C_{fy}Re_x^{\frac{1}{2}} &= -[2(1+R)g' - K\{f'f''g + (f')^2 g'\}]_{\eta=0}, \end{aligned} \tag{12}$$

$$\begin{aligned} Nu\, Re_x^{-\frac{1}{2}} &= -\theta'(0), \\ Sh\, Re_x^{-\frac{1}{2}} &= -\phi'(0). \end{aligned} \tag{13}$$

where $Re_x = \frac{\Omega x^2 \sin\alpha^* (1-st^*)^{-1}}{\nu}$ is the Reynolds number, $Nu = -\frac{[k(\frac{\partial T}{\partial z})]_{z=0}}{T_w - T_\infty}$ and $Sh = -\frac{[\rho D(\frac{\partial C}{\partial z})]_{z=0}}{C_w - C_\infty}$. Note that when K and $R \to 0$ in Eqs. (7) and (8) our problem reduces to the problem of viscous flow [14]. As we are focused to find the self-similar solutions, for this purpose we solve Eqs. (7)–(10) with boundary conditions (11). Self-similar solution means that the solution at different times may be reduced to a single solution i.e., the solution at one value of time t is same to the solution at any other value of time t. This similarity property reduces the number of independent variables to one.

Analytical solutions by homotopy analysis method

In order to proceed for the HAM solutions we choose the base functions of the form

$$\{\eta^k \exp(-n\eta) | k \geqslant 0,\ n \geqslant 0\}, \tag{14}$$

in the form

$$f(\eta) = a_{0,0}^0 + \sum_{n=0}^{\infty}\sum_{k=0}^{\infty} a_{m,n}^k \eta^k \exp(-n\eta), \tag{15}$$

$$g(\eta) = b_{0,0}^0 + \sum_{n=0}^{\infty}\sum_{k=0}^{\infty} b_{m,n}^k \eta^k \exp(-n\eta), \tag{16}$$

$$\theta(\eta) = \sum_{n=0}^{\infty}\sum_{k=0}^{\infty} c_{m,n}^k \eta^k \exp(-n\eta), \tag{17}$$

$$\phi(\eta) = \sum_{n=0}^{\infty}\sum_{k=0}^{\infty} d_{m,n}^k \eta^k \exp(-n\eta), \tag{18}$$

in which $a_{m,n}^k, b_{m,n}^k, c_{m,n}^k, d_{m,n}^k$ are the coefficients. These provide us with solution expressions of $f(\eta)$, $g(\eta)$, $\theta(\eta)$ and $\phi(\eta)$, respectively. The initial approximations f_0, g_0, θ_0 and ϕ_0 along the respective auxiliary linear operators are

$$f_0(\eta) = 0, \tag{19}$$

$$g_0(\eta) = (1-\alpha_1) + (2\alpha_1 - 1)\exp(-\eta), \tag{20}$$

$$\theta_0(\eta) = \exp(-\eta), \tag{21}$$

$$\phi_0(\eta) = \exp(-\eta). \tag{22}$$

$$\pounds_f = \frac{d^3 f}{d\eta^3} - \frac{df}{d\eta}, \tag{23}$$

$$\pounds_g = \frac{d^2 g}{d\eta^2} + \frac{dg}{d\eta}, \tag{24}$$

$$\pounds_\theta = \frac{d^2\theta}{d\eta^2} - \theta, \tag{25}$$

$$\pounds_\phi = \frac{d^2\phi}{d\eta^2} - \phi, \tag{26}$$

The operators given in Eqs. (23)–(26) have the following properties

$$\pounds_f[C_1 + C_2\exp(\eta) + C_3\exp(-\eta)] = 0, \tag{27}$$

$$\pounds_g[C_4 + C_5\exp(-\eta)] = 0, \tag{28}$$

$$\pounds_\theta[C_6\exp(\eta) + C_7\exp(-\eta)] = 0, \tag{29}$$

$$\pounds_\phi[C_8\exp(\eta) + C_9\exp(-\eta)] = 0, \tag{30}$$

where $C_i (i = 1-9)$ are arbitrary constants. Let $p \in [0,1]$ denote an embedding parameter, $\hbar_f$, $\hbar_g$, $\hbar_\theta$ and $\hbar_\phi$ indicate the non -zero auxiliary parameters. The problems at the zeroth order are given by

$$(1-p)\pounds_f[\hat{f}(\eta;p) - \hat{f}_0(\eta)] = p\hbar_f N_f[\hat{f}(\eta;p), \hat{g}(\eta;p), \hat{\theta}(\eta;p), \hat{\phi}(\eta;p)], \tag{31}$$

$$(1-p)\pounds_g[\hat{g}(\eta;p) - \hat{g}_0(\eta)] = p\hbar_g N_g[\hat{f}(\eta;p), \hat{g}(\eta;p)], \tag{32}$$

$$(1-p)\pounds_\theta[\hat{\theta}(\eta;p) - \hat{\theta}_0(\eta)] = p\hbar_\theta N_\theta[\hat{f}(\eta;p), \hat{\theta}(\eta;p)], \tag{33}$$

$$(1-p)\pounds_\phi[\hat{\phi}(\eta;p) - \hat{\phi}_0(\eta)] = p\hbar_\phi N_\phi[\hat{f}(\eta;p), \hat{\phi}(\eta;p)], \tag{34}$$

$$\hat{f}(0;p) = 0 = \hat{f}'(0;p), \quad \hat{g}(0;p) = \alpha_1, \quad \hat{\theta}(0;p) = \hat{\phi}(0;p) = 1, \tag{35}$$

$$\hat{f}'(\infty;p) = 0, \quad \hat{g}(\infty;p) = 1-\alpha_1, \quad \hat{\theta}(\infty;p) = \hat{\phi}(\infty;p) = 0, \tag{36}$$

and the nonlinear operators

$$\begin{aligned} &N_f[\hat{f}(\eta;p), \hat{g}(\eta;p), \hat{\theta}(\eta;p), \hat{\phi}(\eta;p)] \\ &= (1+R)\frac{\partial^3\hat{f}(\eta;p)}{\partial\eta^3} - \hat{f}(\eta;p)\frac{\partial^2\hat{f}(\eta;p)}{\partial\eta^2} + \frac{1}{2}\left(\frac{\partial\hat{f}(\eta;p)}{\partial\eta}\right)^2 \\ &\quad + K\left(8\frac{\partial\hat{f}(\eta;p)}{\partial\eta}\left(\frac{\partial^2\hat{f}(\eta;p)}{\partial\eta^2}\right)^2 - \frac{\partial^2\hat{f}(\eta;p)}{\partial\eta^2}\hat{g}(\eta;p)\frac{\partial\hat{g}(\eta;p)}{\partial\eta}\right) \\ &\quad - 3K\left(\left(\frac{\partial\hat{f}(\eta;p)}{\partial\eta}\right)^2\frac{\partial^3\hat{f}(\eta;p)}{\partial\eta^3} + 2\frac{\partial^3\hat{f}(\eta;p)}{\partial\eta^3}\hat{g}(\eta;p)^2\right) \\ &\quad - 2\lambda_1(\hat{\theta}(\eta;p) + N\hat{\phi}(\eta;p)) - s\left(\frac{\partial\hat{f}(\eta;p)}{\partial\eta} + \frac{1}{2}\eta\frac{\partial^2\hat{f}(\eta;p)}{\partial\eta^2}\right) \\ &\quad - 2[(\hat{g}(\eta;p))^2 - (1-\alpha_1)^2] + 4K\frac{\partial\hat{f}(\eta;p)}{\partial\eta}\left(\frac{\partial\hat{g}(\eta;p)}{\partial\eta}\right)^2, \end{aligned} \tag{37}$$

$$\begin{aligned} N_g[\hat{g}(\eta;p),\hat{f}(\eta;p)] &= (1+R)\frac{\partial^2\hat{g}(\eta;p)}{\partial\eta^2} - \left[\hat{f}(\eta;p)\frac{\partial\hat{g}(\eta;p)}{\partial\eta} - \hat{g}(\eta;p)\frac{\partial\hat{f}(\eta;p)}{\partial\eta}\right] \\ &\quad + s(1-\alpha_1 - \hat{g}(\eta;p) - \frac{1}{2}\eta\frac{\partial\hat{g}(\eta;p)}{\partial\eta}) \\ &\quad + K\left(\frac{1}{4}\left(\frac{\partial^2\hat{f}(\eta;p)}{\partial\eta^2}\right)^2\hat{g}(\eta;p) + 12\frac{\partial\hat{f}(\eta;p)}{\partial\eta}\frac{\partial^2\hat{f}(\eta;p)}{\partial\eta^2}\frac{\partial\hat{g}(\eta;p)}{\partial\eta}\right. \\ &\quad \left. + 3\left(\frac{\partial^2\hat{f}(\eta;p)}{\partial\eta^2}\right)^2\frac{\partial^2\hat{g}(\eta;p)}{\partial\eta^2} - 2\hat{g}(\eta;p)\left(\frac{\partial\hat{g}(\eta;p)}{\partial\eta}\right)^2\right), \end{aligned} \tag{38}$$

$$\begin{aligned} N_\theta[\hat{\theta}(\eta;p),\hat{f}(\eta;p)] &= \frac{1}{Pr}\frac{\partial^2\hat{\theta}(\eta;p)}{\partial\eta^2} \\ &\quad - \left(\hat{f}(\eta;p)\frac{\partial\hat{\theta}(\eta;p)}{\partial\eta} - \frac{1}{2}\frac{\partial\hat{f}(\eta;p)}{\partial\eta}\hat{\theta}(\eta;p)\right) \\ &\quad - s(2\hat{\theta}(\eta;p) + \frac{1}{2}\eta\frac{\partial\hat{\theta}(\eta;p)}{\partial\eta}), \end{aligned} \tag{39}$$

$$\begin{aligned} N_\phi[\hat{\phi}(\eta;p),\hat{f}(\eta;p)] &= \frac{1}{Sc}\frac{\partial^2\hat{\phi}(\eta;p)}{\partial\eta^2} - (\hat{f}(\eta;p)\frac{\partial\hat{\phi}(\eta;p)}{\partial\eta} \\ &\quad - \frac{1}{2}\frac{\partial\hat{f}(\eta;p)}{\partial\eta}\hat{\phi}(\eta;p)) \\ &\quad - s\left(2\hat{\phi}(\eta;p) + \frac{1}{2}\eta\frac{\partial\hat{\phi}(\eta;p)}{\partial\eta}\right). \end{aligned} \tag{40}$$

For $p = 0$ and $p = 1$, we have

$$\hat{f}(\eta;0) = f_0(\eta), \quad \hat{f}(\eta;1) = f(\eta), \tag{41}$$
$$\hat{g}(\eta;0) = g_0(\eta), \quad \hat{g}(\eta;1) = g(\eta), \tag{42}$$
$$\hat{\theta}(\eta;0) = \theta_0(\eta), \quad \hat{\theta}(\eta;1) = \theta(\eta), \tag{43}$$
$$\hat{\phi}(\eta;0) = \phi_0(\eta), \quad \hat{\phi}(\eta;1) = \phi(\eta). \tag{44}$$

When p varies from 0 to 1, then the initial guesses vary from $f_0(\eta)$, $g_0(\eta)$, $\theta_0(\eta)$, $\phi_0(\eta)$ to $f(\eta)$, $g(\eta)$, $\theta(\eta)$, $\phi(\eta)$, respectively. Due to Taylor's series with respect to p, we have by Taylor's theorem

$$\hat{f}(\eta;p) = f_0(\eta) + \sum_{m=1}^{\infty} f_m(\eta)p^m, \tag{45}$$
$$\hat{g}(\eta;p) = g_0(\eta) + \sum_{m=1}^{\infty} g_m(\eta)p^m, \tag{46}$$
$$\hat{\theta}(\eta;p) = \theta_0(\eta) + \sum_{m=1}^{\infty} \theta_m(\eta)p^m, \tag{47}$$
$$\hat{\phi}(\eta;p) = \phi_0(\eta) + \sum_{m=1}^{\infty} \phi_m(\eta)p^m, \tag{48}$$

$$\begin{aligned} f_m(\eta) &= \tfrac{1}{m!}\tfrac{\partial^m \hat{f}(\eta;p)}{\partial \eta^m}\Big|_{p=0}, g_m(\eta) = \tfrac{1}{m!}\tfrac{\partial^m \hat{g}(\eta;p)}{\partial \eta^m}\Big|_{p=0}, \\ \theta_m(\eta) &= \tfrac{1}{m!}\tfrac{\partial^m \hat{\theta}(\eta;p)}{\partial \eta^m}\Big|_{p=0}, \phi_m(\eta) = \tfrac{1}{m!}\tfrac{\partial^m \hat{\phi}(\eta;p)}{\partial \eta^m}\Big|_{p=0}, \end{aligned} \tag{49}$$

and

$$f(\eta) = f_0(\eta) + \sum_{m=1}^{\infty} f_m(\eta), \tag{50}$$
$$g(\eta) = g_0(\eta) + \sum_{m=1}^{\infty} g_m(\eta). \tag{51}$$
$$\theta(\eta) = \theta_0(\eta) + \sum_{m=1}^{\infty} \theta_m(\eta). \tag{52}$$
$$\phi(\eta) = \phi_0(\eta) + \sum_{m=1}^{\infty} \phi_m(\eta). \tag{53}$$

The mth-order deformation problems satisfy the following expressions

$$\pounds_f[f_m(\eta) - \chi_m f_{m-1}(\eta)] = \hbar_f R_m^f(\eta), \tag{54}$$
$$\pounds_g[g_m(\eta) - \chi_m g_{m-1}(\eta)] = \hbar_g R_m^g(\eta), \tag{55}$$
$$\pounds_\theta[\theta_m(\eta) - \chi_m \theta_{m-1}(\eta)] = \hbar_\theta R_m^\theta(\eta), \tag{56}$$
$$\pounds_\phi[\phi_m(\eta) - \chi_m \phi_{m-1}(\eta)] = \hbar_\phi R_m^\phi(\eta), \tag{57}$$
$$f_m(0) = f'_m(0) = g_m(0) = \theta_m(0) = \phi_m(0) = 0, \tag{58}$$
$$f'_m(\infty) = g_m(\infty) = \theta_m(\infty) = \phi_m(\infty) = 0, \tag{59}$$

$$\begin{aligned} R_m^f(\eta) &= (1+R)f'''_{m-1} - 2\lambda_1(\theta_{m-1} + N\phi_{m-1}) - s\left(f'_{m-1} + \frac{1}{2}\eta f'''_{m-1}\right) \\ &\quad - \sum_{k=0}^{m-1}\left(f_k f''_{m-1-k} + \frac{1}{2}f'_k f'_{m-1-k}\right) - 2\left[\sum_{k=0}^{m-1} g_k g_{m-1-k} - (1-\alpha_1)^2\right] \\ &\quad + K\sum_{k=0}^{m-1}\left(8f''_{m-1-k}\sum_{l=0}^{k} f''_{k-l}f'_l - f_{m-1} - k''\sum_{l=0}^{k} f''_{k-l}g'_l\right. \\ &\quad \left. + 4f'_{m-1-k}\sum_{l=0}^{k} g_{k-l}g_l - 3f_{m-1-k}\sum_{l=0}^{k} f_{k-l}f_l + 2f'''_{m-1-k}\sum_{l=0}^{k} g_{k-l}g_l\right), \end{aligned} \tag{60}$$

$$\begin{aligned} R_m^g(\eta) &= (1+R)g''_{m-1} - \sum_{k=0}^{m-1}\left[f_k g'_{m-1-k} - g_k f'_{m-1-k}\right] \\ &\quad + s\left(1 - \alpha_1 - g_{m-1} - \frac{1}{2}\eta g'_{m-1}\right) \\ &\quad + K\sum_{k=0}^{m-1}\left(\frac{1}{4}g_{m-1-k}\sum_{l=0}^{k} f''_{k-l}f''_l + 12f'_{m-1-k}\sum_{l=0}^{k} f''_{k-l}g'_l\right. \\ &\quad \left. + 3g''_{m-1-k}\sum_{l=0}^{k} f''_{k-l}f'_l - 2g_{m-1-k}\sum_{l=0}^{k} g'_{k-l}g'_l\right), \end{aligned} \tag{61}$$

$$R_m^\theta(\eta) = \frac{1}{Pr}\theta''_{m-1} - \sum_{k=0}^{m-1}\left[f_k\theta'_{m-1-k} - \frac{1}{2}\theta_k f'_{m-1-k}\right] - s\left(2\theta_{m-1} + \frac{1}{2}\eta\theta'_{m-1}\right), \tag{62}$$
$$R_m^\phi(\eta) = \frac{1}{Sc}\phi''_{m-1} - \sum_{k=0}^{m-1}\left[f_k\phi'_{m-1-k} - \frac{1}{2}\phi_k f'_{m-1-k}\right] - s\left(2\phi_{m-1} + \frac{1}{2}\eta\phi'_{m-1}\right), \tag{63}$$

$$\chi_m = \begin{cases} 0 & m \leqslant 1, \\ 1 & m > 1. \end{cases} \tag{64}$$

The general solutions of Eqs. (54)–(59) are

$$f_m(\eta) = f_m^*(\eta) + C_1 + C_2\exp(\eta) + C_3\exp(-\eta), \tag{65}$$
$$g_m(\eta) = g_m^*(\eta) + C_4 + C_5\exp(-\eta), \tag{66}$$
$$\theta_m(\eta) = \theta_m^*(\eta) + C_6\exp(\eta) + C_7\exp(-\eta), \tag{67}$$
$$\phi_m(\eta) = \phi_m^*(\eta) + C_8\exp(\eta) + C_9\exp(-\eta), \tag{68}$$

in which $f_m^*(\eta), g_m^*(\eta), \theta_m^*(\eta)$ and $\phi_m^*(\eta)$ denote the special solutions of (54)–(58) and the integral constants $C_i (i = 1 - 9)$ are determined

Table 1
Total averaged squared residual errors using single optimal convergence control parameter c_0.

m	c_0	ε_m^t
2	−0.84	1.12×10^{-2}
4	−0.65	3.78×10^{-3}
6	−0.54	2.39×10^{-3}
8	−0.51	2.06×10^{-3}

Table 2
Average squared residual errors using Table 1.

m	2	4	6	8
ε_m^f	1.86×10^{-4}	1.83×10^{-4}	1.79×10^{-4}	1.77×10^{-4}
ε_m^g	2.85×10^{-3}	1.61×10^{-3}	1.16×10^{-3}	9.96557×10^{-4}
ε_m^θ	4.39×10^{-3}	1.08×10^{-3}	5.74×10^{-4}	4.85×10^{-4}
ε_m^ϕ	3.87×10^{-3}	9.12×10^{-4}	4.77×10^{-4}	4.03×10^{-4}

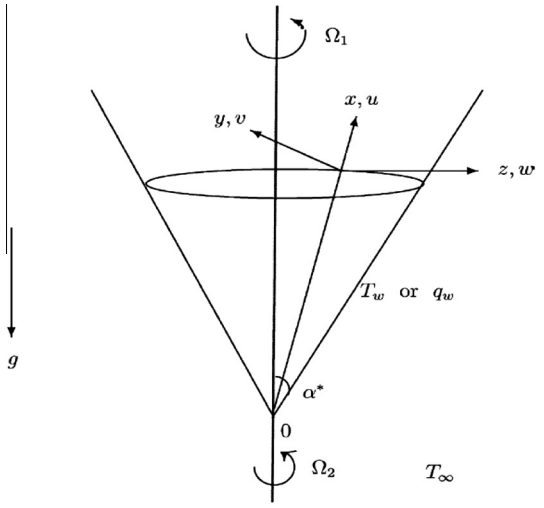

Fig. 1. Schematic diagram and coordinate system.

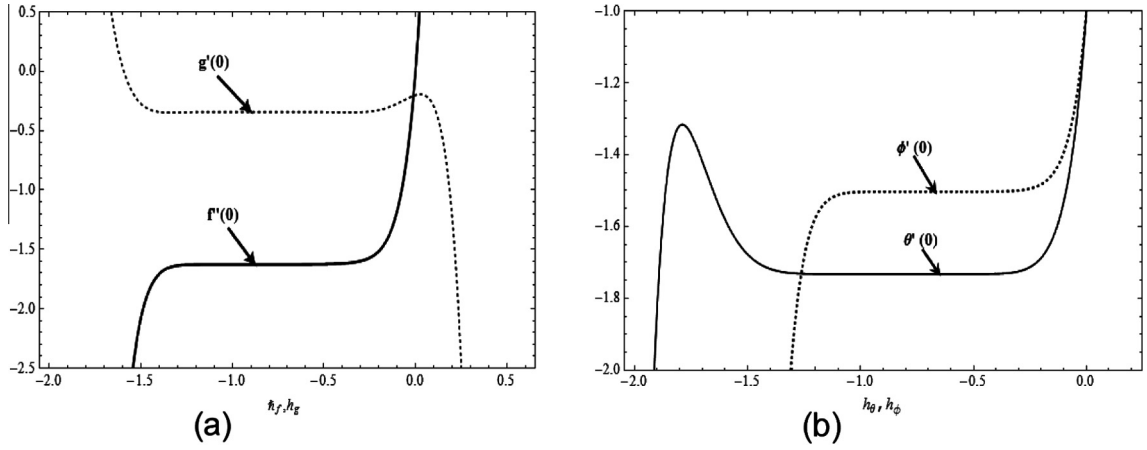

Fig. 2. (a) and (b) h-curves for $f''(0)$, $g'(0)$, $\theta'(0)$ and $\phi'(0)$ for 10th order of approximations, respectively.

by employing the boundary conditions (59) and (60). It is noted that to satisfy the boundary conditions at infinity, we must set C_2, C_6 and C_8 equal to zero. Note that Eqs. (54)–(58) can be solved by Mathematica one after the other in the order $m = 1,2,3,\ldots$.

Optimal convergence-control parameters

It is seen that the series solutions obtained by HAM, contain the non-zero auxiliary parameters c_0^f, c_0^g, c_0^θ and c_0^ϕ, which determine the convergence-region and rate of the homotopy series solutions. In order to determine the optimal values of c_0^f, c_0^g, c_0^θ, and c_0^ϕ, it is used here the so-called average residual error defined by Liao [23].

$$\varepsilon_m^f = \frac{1}{j+1}\sum_{i=0}^{j}\left[\mathbf{N}_f\left(\sum_{n=0}^{m}\hat{f}(\eta),\sum_{n=0}^{m}\hat{g}(\eta),\sum_{n=0}^{m}\hat{\theta}(\eta),\sum_{n=0}^{m}\hat{\phi}(\eta)\right)_{y=i\delta y}\right]^2 dy \quad (69)$$

$$\varepsilon_m^g = \frac{1}{j+1}\sum_{i=0}^{j}\left[\mathbf{N}_g\left(\sum_{n=0}^{m}\hat{f}(\eta),\sum_{n=0}^{m}\hat{g}(\eta),\right)_{y=i\delta y}\right]^2 dy \quad (70)$$

$$\varepsilon_m^\theta = \frac{1}{j+1}\sum_{i=0}^{j}\left[\mathbf{N}_\theta\left(\sum_{n=0}^{m}\hat{f}(\eta),\sum_{n=0}^{m}\hat{\theta}(\eta),\sum_{n=0}^{m}\hat{\phi}(\eta)\right)_{y=i\delta y}\right]^2 dy \quad (71)$$

$$\varepsilon_m^\phi = \frac{1}{j+1}\sum_{i=0}^{j}\left[\mathbf{N}_\phi\left(\sum_{n=0}^{m}\hat{f}(\eta),\sum_{n=0}^{m}\hat{\theta}(\eta),\sum_{n=0}^{m}\hat{\phi}(\eta)\right)_{y=i\delta y}\right]^2 dy \quad (72)$$

Following Liao [23]

$$\varepsilon_m^t = \varepsilon_m^f + \varepsilon_m^g + \varepsilon_m^\theta + \varepsilon_m^\phi \quad (73)$$

where ε_m^t is the total squared residual error, $\delta y = 0.5$ and $J = 20$. Total average squared residual error is minimized by using symbolic computation software Mathematica. We have directly applied the command **Minimize** to obtain the corresponding local optimal convergence control parameters. Tables 1 and 2 are presented for the case of single optimal convergence control parameter. It is found that the averaged squared residual errors and total averaged squared residual errors are getting smaller and smaller as we increase the order of approximation. Therefore, the optimal homotopy analysis method gives us relaxation to select any set of local convergence control parameters to obtain convergent results.

Results and discussion

The solutions of highly nonlinear coupled ordinary differential equations of the concerning flow problem are carried out by a famous analytical tool namely the optimal homotopy analysis method. It was proposed by Liao [23]. We have seen that the series solutions (52)–(55) contain the non-zero auxiliary parameters $\hbar_f$, $\hbar_g$, $\hbar_\theta$ and $\hbar_\phi$. These auxiliary parameters adjust and control the convergence of the series solutions. For admissible values of the auxiliary parameters $\hbar_f$, $\hbar_g$, $\hbar_\theta$ and $\hbar_\phi$, $\hbar$-curve is plotted for 15th-order of approximations. Fig. 2(a) and (b) depicts that the range for the acceptable values of $\hbar_f$, $\hbar_g$,$\hbar_\theta$ and $\hbar_\phi$ are $-1.2 \leqslant \hbar_f \leqslant -0.4$, $-1.3 \leqslant \hbar_g \leqslant -0.3$, $-1.2 \leqslant \hbar_\theta \leqslant -0.3$, $-1.3 \leqslant \hbar_\phi \leqslant -0.3$. It is apparent from the Tables 1 and 2 that, the obtained optimal values are well within the convergence region as shown in Fig. 2(a) and (b). An excellent agreement of our present analytical results with the previous literature [14] is given in Table 3. Further the influences of ratio of angular velocities of the cone and the fluid α_1, ratio of the buoyancy forces N, flow parameters K and R on the velocity, temperature and concentration fields are presented in graphical and tabular forms. These influences have been analyzed in Figs. 3–9. The variation of both velocities (i.e., tangential and azimuthal) for combined effects of α_1 and λ_1 is sketched in Fig. 3(a) and (b), respectively. The direction of both the fluid and the cone is same when rotating with an equal angular velocity for $\alpha_1 = 0.5$. The positive Buoyancy force i.e., $\lambda_1 = 1$ which behaves as favorable pressure gradient is responsible for the flow. For $\alpha_1 > 0.5$, the tangential velocity $-f'(\eta)$ has an increasing magnitude, but the azimuthal velocity $g(\eta)$ reduces. While for $\alpha_1 < 0.5$ the behavior is

Table 3
Comparison of OHAM results and numerical results when $K = R = 0$.

Pr	Sc	Present results				Numerical results [14]			
		$C_{fx}Re_x^{\frac{1}{2}}$	$C_{fy}Re_x^{\frac{1}{2}}$	$NuRe_x^{-\frac{1}{2}}$	$ShRe_x^{-\frac{1}{2}}$	$C_{fx}Re_x^{\frac{1}{2}}$	$C_{fy}Re_x^{\frac{1}{2}}$	$NuRe_x^{-\frac{1}{2}}$	$ShRe_x^{-\frac{1}{2}}$
0.7	0.22	1.55441	−0.18622	0.92497	0.52520	1.55441	−0.18622	0.92497	0.52520
	0.60	1.39263	−0.21528	0.90106	0.83546	1.39265	−0.21528	0.90102	0.83549
	0.94	1.31331	−0.22757	0.89011	1.02810	1.31338	−0.22757	0.89011	1.02816
	2.57	1.13111	0.25133	0.86677	1.63912	1.13111	0.25133	0.86679	1.63912

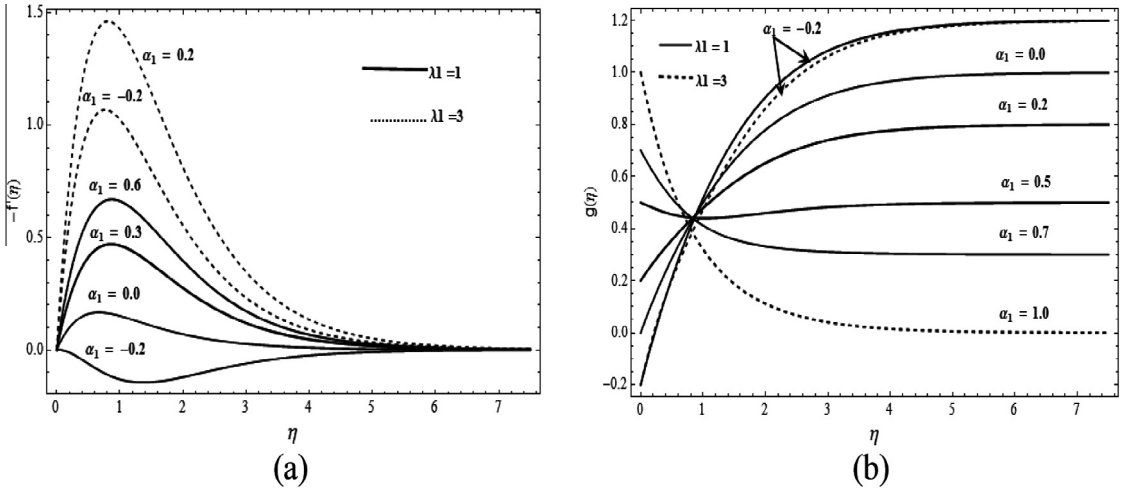

Fig. 3. (a) and (b) Effects of α_1 on velocities-$f'(\eta)$ and $g(\eta)$.

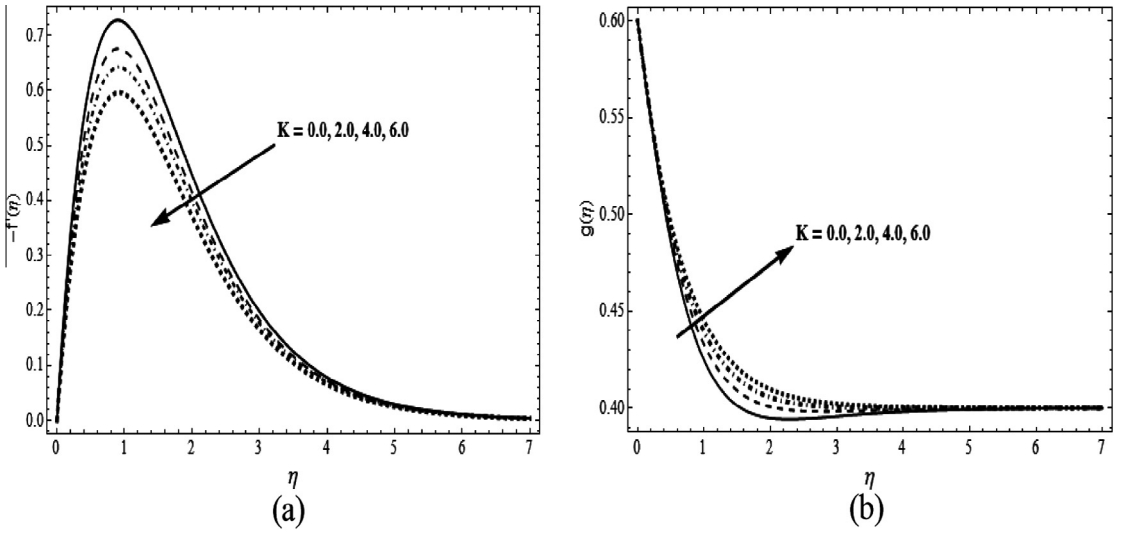

Fig. 4. (a) and (b) Effects of K on velocities-$f'(\eta)$ and $g(\eta)$.

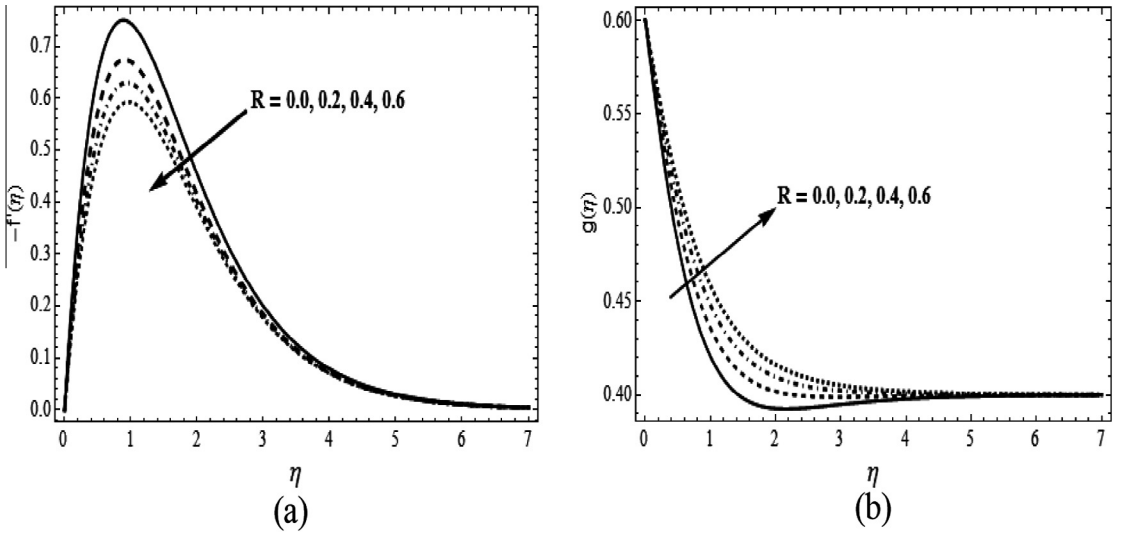

Fig. 5. (a) and (b) Effects of R on velocities-$f'(\eta)$ and $g(\eta)$.

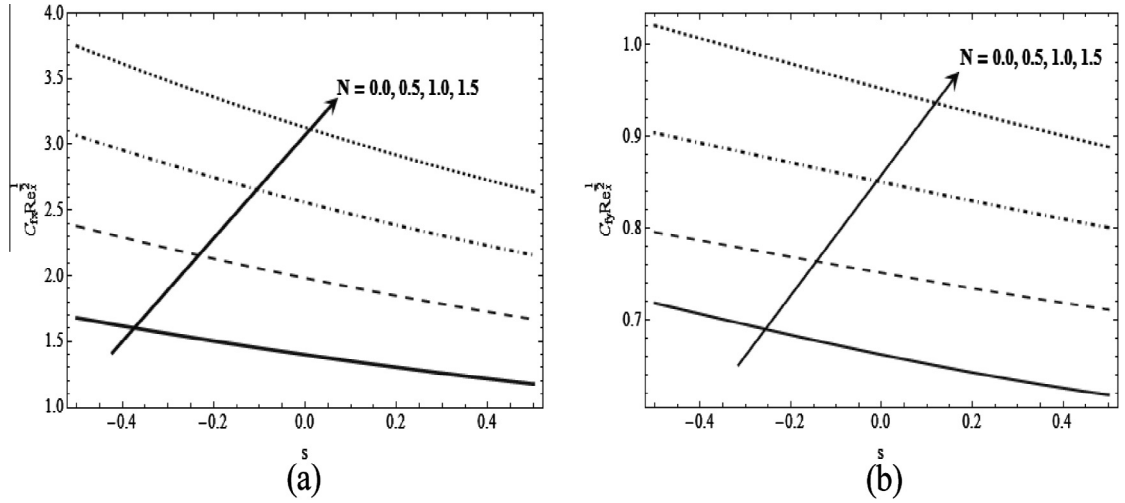

Fig. 6. (a) and (b) Effects of N on $C_{fx}Re_x^{\frac{1}{2}}$ and $C_{fy}Re_x^{\frac{1}{2}}$.

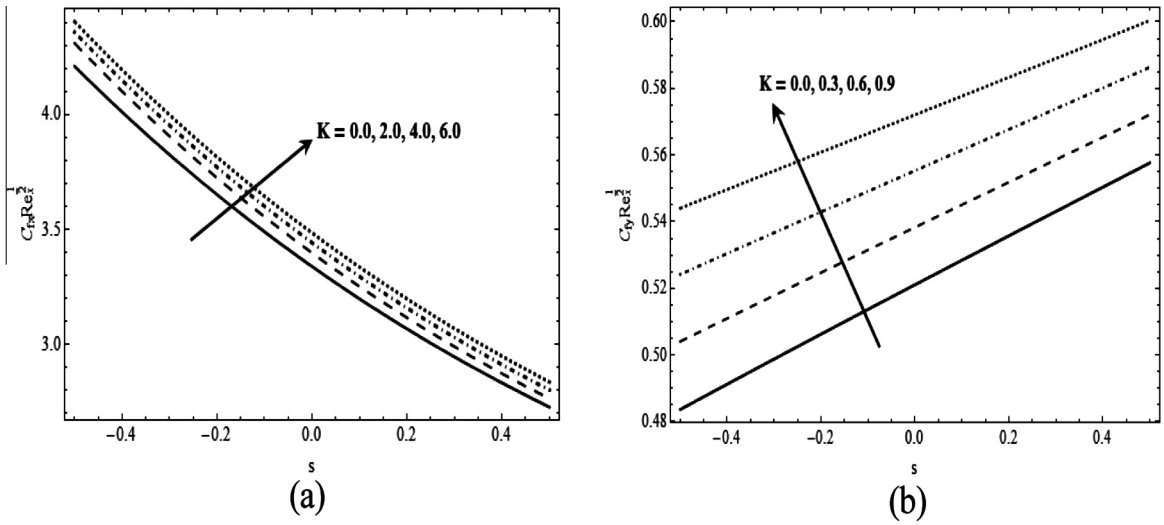

Fig. 7. (a) and (b) Effects of K on $C_{fx}Re_x^{\frac{1}{2}}$ and $C_{fy}Re_x^{\frac{1}{2}}$.

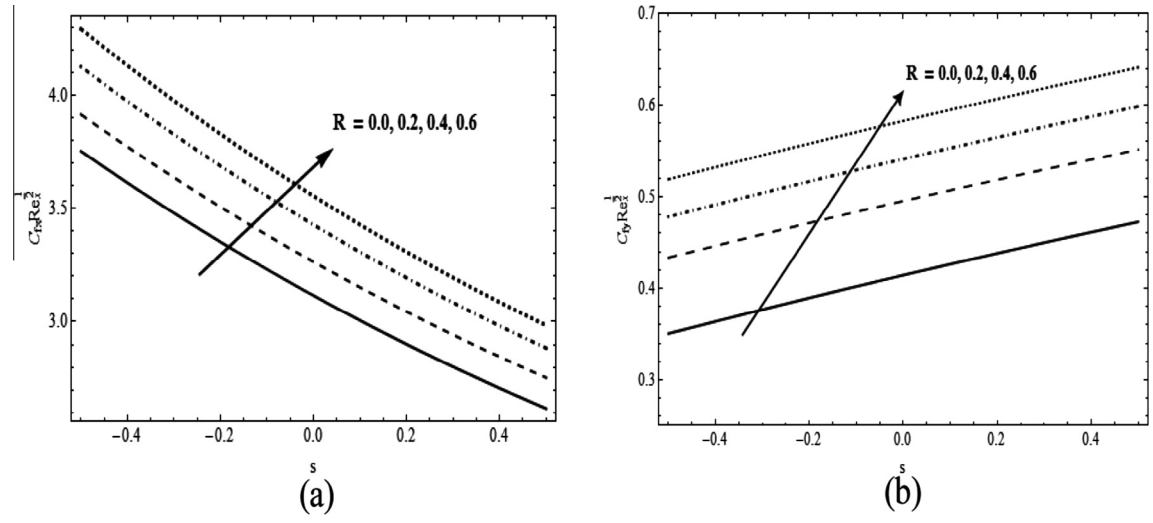

Fig. 8. (a) and (b) Effects of R on $C_{fx}Re_x^{\frac{1}{2}}$ and $C_{fy}Re_x^{\frac{1}{2}}$.

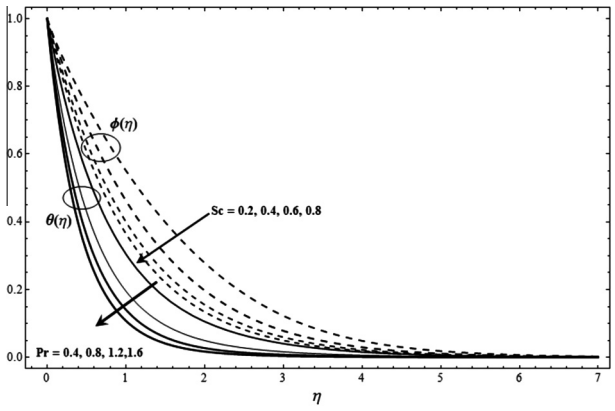

Fig. 9. Effects of *Pr* and *Sc* on temperature $\theta(\eta)$ and concentration $\phi(\eta)$, respectively.

Table 4
Numerical values of skin friction coefficients, Nusselt and Sherwood number for different values of flow parameters.

K	R	$C_{fx}Re_x^{\frac{1}{2}}$	$C_{fy}Re_x^{\frac{1}{2}}$	$NuRe_x^{-\frac{1}{2}}$	$ShRe_x^{-\frac{1}{2}}$
0.0	0.1	2.71214	0.58070	0.90461	1.02345
2.0		2.69289	0.69232	0.88873	1.00725
4.0		2.67005	0.79226	0.87698	0.99475
6.0		2.62419	0.88221	0.86253	0.98515
0.5	0.0	2.63619	0.84054	0.91242	1.82485
	0.2	2.79437	0.87245	0.89739	0.89831
	0.4	2.91897	0.89859	0.88517	0.88660
	0.6	2.99338	0.92283	0.87519	0.87660

opposite. The asymptotic behavior at the edge of boundary layer of both velocities is noticed for $\alpha_1 < 0$ and $\lambda_1 = 1$. Physically these oscillations are caused by surplus convection of angular momentum present in the boundary layer. Fig. 4(a) and (b) depict the behavior of tangential velocity $-f'(\eta)$ and azimuthal velocity $g(\eta)$ on various values of K, respectively. It is illustrated that the tangential velocity $-f'(\eta)$ decreases as the values of K get higher. On the other hand the azimuthal velocity $g(\eta)$ shows an increasing attitude. In Fig. 5(a) and (b) the effects of flow parameter R have been plotted for tangential velocity $-f'(\eta)$ and azimuthal velocity $g(\eta)$, respectively. It is clear from the figure that the variation of both velocities is opposite. Fig. 6(a) and (b) give the variations of ratio of the buoyancy forces N on the skin friction coefficients in both directions (i.e., tangential and azimuthal). It is found that both the skin friction coefficients are increasing functions of N. Tangential and azimuthal skin friction coefficients increase by increasing flow parameter K and R (see Figs. 7 and 8), respectively. The effects of Prandtl number *Pr* and Schmidt number *Sc* on temperature and concentration profiles are shown in Fig. 9. Both the thermal and concentrated boundary layer decreases with an increase in Prandtl number *Pr* and Schmidt number *Sc*, respectively. Physically higher Prandtl number *Pr* fluid has a lower thermal conductivity which results in thinner thermal boundary layer and thus the rate of heat transfer grows up. For engineering phenomenon, the heat transfer rate should be small. This can be maintained by keeping the low temperature difference between the surface and the free stream fluid, using a low Prandtl number fluid, keeping the surface at a constant temperature instead of at a constant heat flux, and by applying the buoyancy force in the opposing direction to that of forced flow. The influences of flow parameters K and R on skin friction coefficients, Nusselt number and Sherwood number in a tabular form are given in Table 4. It is found that skin friction coefficients increase for R, but other physical quantities show an opposite variation for increasing values of K and R.

Remarks

We have inspected the unsteady mixed convection flow of rotating Eyring–Powell fluid on a rotating cone in the presence of heat and mass transfer. The non-dimensional differential equations are solved by the optimal homotopy analysis method. The present results are found to be in decent agreement with the prior results of published work. The important results are concluded as follows:

- The effects of ratio of angular velocities α_1 are significant on both velocities.
- The tangential velocity $-f'(\eta)$ and azimuthal velocity $g(\eta)$ have opposite behavior for flow parameter K and R.
- The increase in Prandtl number *Pr* and Schmidt number *Sc* causes a reduction in the thermal and concentrated boundary layer, respectively.
- The skin friction coefficients increase its magnitude due to an increase in ratio of buoyancy forces N and flow parameter R, but decreases with increasing K.
- The Nusselt and Sherwood numbers are decreasing function of K and R.

References

[1] Dumn JE, Rajagopal KR. Fluids of differential type: critical review and thermodynamic analysis. Int J Eng Sci 1995;33:689.
[2] Patel M, Timol MG. The stress-strain relationship for visco-inelastic non-Newtonian fluids. Int J Appl Math Mech 2010;6:79.
[3] Kapur JN, Bhatt BS, Sacheti NC. Non-Newtonian fluid flows. Meerut, India: Pragati Prakashan; 1982.
[4] Fetecau C, Fetecau C. Starting solutions for some unsteady unidirectional flows of a second grade fluid. Int J Eng Sci 2005;43:781.
[5] Akbar Noreen Sher, Nadeem S, Lee Changhoon, Khan Zafar Hayat, Haq Rizwan Ul. Numerical study of Williamson nano fluid flow in an asymmetric channel. Results Phys 2013;3:161.
[6] Akbar Noreen Sher, Nadeem S. Thermal and velocity slip effects on the peristaltic flow of a six constant Jeffrey's fluid model. Int J Heat Mass Trans 2012;55:3964.
[7] Ellahi R. Effects of the slip boundary condition on non-Newtonian flows in a channel. Commun Nonlinear Sci Nume Simul 2009;14:1377.
[8] Nadeem S, Haq RU, Lee C. MHD flow of a Casson fluid over an exponentially shrinking sheet. Sci Iran 2012;19:1550.
[9] Qasim M. Heat and mass transfer in a Jeffrey fluid over a stretching sheet with heat source/sink. Alexandria Eng J 2013;52(4):571.
[10] Hering RG, Grosh RJ. Mixed convection along a vertical cone. ASME J Heat Transfer 1963;85:29.
[11] Himasekhar K, Sarma PK, Janardhan K. Laminar mixed convection from a vertical rotating cone. Int Commun Heat Mass Transfer 1989;16:99.
[12] Kumari M, Pop I, Nath G. Mixed convection along a vertical cone. Int Commun Heat Mass Transfer 1989;16:247.
[13] Anilkumar D, Roy S. Unsteady mixed convection from a rotating cone in a rotating fluid due to the combined effects of thermal and mass diffusion. Int J Heat Mass Transfer 2004;47:1673.
[14] Anilkumar D, Roy S. Unsteady mixed convection flow on a rotating cone in a rotating fluid. Appl Math Comput 2004;155:545.
[15] Ishak A, Nazar R, Bachok N, Pop I. MHD mixed convection flow near the stagnation-point on a vertical permeable surface. Physica A Stat Mech Appl 2010;389:40.
[16] Wang CY. Boundary layers on rotating cones, discs and axisymmetric surfaces with a concentrated heat source. Acta Mech 1990;81:245.
[17] Yih KA. Mixed convection about a cone in a porous medium: the entire regime. Int Commun Heat Mass Transfer 1999;26:1041.
[18] Powell RE, Eyring H. Mechanism for relaxation theory of viscosity. Nature 1944;154:427.
[19] Akbar NS, Nadeem S. Characteristics of heating scheme and mass transfer on the peristaltic flow for an Eyring–Powell fluid in an endoscope. Int J Heat Mass Transfer 2012;55:375.
[20] Petal M, Timol MG. Numerical treatment of Powell–Eyring fluid flow using method of satisfaction of boundary condition. Appl Numer Math 2009;59:2584.
[21] Sirohi V, Timol MG, Kalathia NL. Numerical treatment of Powell–Eyring fluid flow past a 90 degree wedge. J Energy Heat Mass Transfer 1984;6:219.
[22] Liao SJ. Beyond perturbation: introduction to the homotopy analysis method. Boca Raton: Chapman & Hall/CRC Press; 2003.
[23] Liao SJ. An optimal homotopy-analysis approach for strongly nonlinear differential equations. Comm Nonlinear Sci Numer Simulat 2010;15:2003.

[24] Liao SJ. A general approach to get series solution of non-similarity boundary layer flows. Commun Nonlinear Sci Numer Simul 2009;14:44.
[25] Liao SJ. Notes on the homotopy analysis method: some definitions and theorems. Commun Nonlinear Sci Numer Simul 2009;14:983.
[26] Abbasbandy S. Approximate solution of the nonlinear model of diffusion and reaction catalysts by means of the homotopy analysis method. Chem Eng J 2008;136:144.
[27] Nadeem S, Abbasbandy S, Hussain M. Series solutions of boundary layer flow of a micropolar fluid near the stagnation point towards a shrinking sheet. Zeitschrift für Naturforschung 2009;64a:1.
[28] Nadeem S, Saleem S. Analytical treatment of unsteady mixed convection MHD flow on a rotating cone in a rotating frame. J Taiwan Inst Chem Eng 2013;44:596.
[29] Malik MY, Hussain A, Nadeem S. Analytical treatment of an Oldroyd-8 constant fluid between the coaxial cylinder with variable viscosity. Commun Theor Phys 2011;56:933.
[30] Abbasbandy S. The application of homotopy analysis method to nonlinear equations arising in heat transfer. Phys Lett A 2006;60:109.
[31] Nadeem S, Saleem S. Analytical study of rotating non-Newtonian nanofluid on a rotating cone. J Thermophy Heat Trans 2014. http://dx.doi.org/10.2514/1.T4145.
[32] Ellahi R. The effects of MHD and temperature dependent viscosity on the flow of non-Newtonian nanofluid in a pipe: analytical solutions. Appl Math Model 2013;37:1451.
[33] Ellahi R, Riaz A. Analytical solutions for MHD flow in a third-grade fluid with variable viscosity. Math Comput Model 2010;52:1783.